Supplemental Data

Supplemental Materials and Methods

Neural Colony-forming Cell assay was performed using the Neural Colony-forming Cell assay Kit (StemCell Tech., cat# 05740) based on the manufacturer's protocol. Briefly, 2,500 dissociated neurosphere cells were plated in 1.5 ml of collagen/medium/EGF and the number and size of newly formed neurospheres were quantified after 21 days.

Antibodies used for Immunoblot analysis. Sox-2 (rabbit polyclonal, Abcam Ab59776, Cambridge, MA), p53 (FL-293), p21 (C-19), cyclin A (C-19), cyclin D1 (C-20), cyclin E (M-20), cyclin B1 (M-20) (all Santa Cruz Biotechn., Santa Cruz CA), MAPK (mouse monoclonal, Millipore 05-157, Billerica, MA).

Antibodies used for immunohistochemistry

BrdU (1;300, rat anti-BrdU, Serotec)

GFAP (1:1000, Abcam, ab7260)

CNPase (1:100, clone11-5B, Sigma # C5922)

Ki67 (1:25, Dako, TEC-3, M7249)

Sox2 (1:1000, Chemicon AB5603)

phospho-Tau (1: 100, mouse monoclonal, clones CP13 and PHF1, gift from Peter Davies, Albert Einstein University, New York)

Cleaved Casp3 (1:200, Cell Signaling, 5A1E, #9664)

NeuN (1:500, Millipore, MAB377)

Map2a,b (1:500, Neomarkers, MS-249-S0)

SA-β-Galactosidase staining. SA-β-Galactosidase staining was perfomed as previously described (1)**.** Cells from freshly dissociated neurospheres generated from WT and p73-/- Nestin-GFP mice at E14 and P0 were seeded on poly-D-lysine coated glass slides and briefly allowed to attach. Cells were washed in PBS, fixed with 0.2% glutaraldehyde for 5 minutes, washed 4 times in PBS and incubated at 37°C (in the absence of CO2) with freshly prepared senescence-associated β-gal solution (2). Twelve hours later pictures were taken and positive versus total number of GFP-positive cells were counted in 20 random 20x-fields per sample (minimum of 1000 cells each). The percentage of SA-β-gal positive cells per field was averaged and plotted.

Neuroanatomy. Heads of mouse embryos were removed, the skin peeled back to improve fixation and fixed in 4% paraformaldehyde for 20 hrs. Adult mice were anesthetized with 2.5% Avertin and transcardially perfused with PBS followed by 4% paraformaldehyde. Tissues were washed 3x in PBS, 1 hr each, and the tissue was dehydrated in ethanol-isopropanol-xylol alcohol series. Tissues were processed and embedded in paraffin. Brains were serially

sectioned (3 µm) in the coronal plane and stained by H&E or antibodies. Bielschovsky's silver stains were performed per manufacturer's instruction (PolyScientific, Bayshore, NY).

Immunohistochemistry. After antigen retrieval (boiling for 15 min in 10 mM citrate buffer pH 6.0), 3 µm paraffin-embedded sections were incubated with primary antibody overnight at 4ºC. After incubation in biotinylated secondary antibody (GE Healthcare, 1:200) followed by Extravidin-Peroxidase (Sigma E2886, 1:1000), sections were stained with diaminobenzidine and counterstained with Mayers Haemalaun solution. Images were acquired on a Zeiss Axio Scope MAT with AxioVision Rel. 4.8 software. Image analysis and quantification of immunohistochemistry was performed with custom-made scripts for 'ImageJ' (http://rsbweb.nih.gov/ij/). Data were analyzed using 'R' statistical computing language (http://www.r-project.org). For quantification of Brdu, 3-6 coronal brain sections per animal from corresponding stereotaxic planes were analyzed by calculating the percentage of positive area above a standardized threshold.

Quantitative RT-PCR. Semiquantitative and quantitative real-time RT-PCR were performed using whole cell RNAs prepared from neurospheres as previously described (3). Total RNA was extracted using Trizol reagent (Invitrogen)). cDNA was prepared with SuperScript II First-Strand Synthesis SuperMix for qRT-PCR (Invitrogen). Real-time PCR was performed according to the manufacturers' specifications using SYBR Green Realtime PCR Detection System (Opticon II). Samples were analyzed in duplicates and were normalized to GAPDH for each reaction.

qRT-PCR primers used in this study:

TAp73
forward: 5'-GAGCACCTGTGGAGTTCTCTAGAG-3'
reverse: 5' GGTATTGGAAGGGATGACAGGCG-3'

ΔNp73
forward: 5'-GATGCAGCCAGTTGACAGAA-3'
reverse: 5'-GGTATTGGAAGGGATGACAGGCG-3'

pan p73
forward: 5'-GGGCCATGCCTGTCTACAAGAA-3'
reverse: 5'-GATGGTGGTAAATTCTGTTCC-3'

Sox2
forward: 5'-GGCAGCTACAGCATGATGCAGGAGC-3'
reverse: 5'-CTGGTCATGGAGTTGTACTGCAGG-3'

Sox3
forward: 5'-CACAACTCCGAGATCAGCAA-3'
reverse: 5'-GTCCTTCTTGAGCAGCGTCT-3'

Notch1
forward: 5'-CCCTTGCTCTGCCTAACGC-3'

reverse: 5'- GGAGTCCTGGCATCGTTGG-3'

Notch 2
forward: 5'-ATGTGGACGAGTGTCTGTTGC-3'
reverse: 5'-GGAAGCATAGGCACAGTCATC-3'

Notch 3
forward: 5'-TGCCAGAGTTCAGTGGTGG-3'
reverse: 5'-CACAGGCAAATCGGCCATC-3'

Hes5
forward: 5' – AGTCCCAAGGAGAAAAACCGA-3'
reverse: 5'-GCTGTGTTTCAGGTAGCTGAC-3'

Hey2
forward: 5'- TCTGCCAAGTTAGAAAAGGCTG -3'
reverse: 5'- CAAGAGCATGGGCATCAAAGTA -3'

Jag1
forward: 5'-CAAAGTGTGCCTCAAGGAGTATCAG-3'
reverse: 5'-TCCACCAGCAAAGTGTAGGACCTC-3'

Jag2
forward: 5'-CAAGTTGTGTGACGAGTGTGTCCC-3'
reverse: 5'-TTGCCCAAGTAGCCATCTGG-3'

Nestin
forward: 5'-GTCGCTTAGAGGTGCAGCAG-3'
reverse: 5'-TTCCAGGATCTGAGCGATCT-3'

GAPDH
forward: 5'-TCCTGCACCACCAACTGCTT-3'
reverse: 5'-GTCTTCTGGGTGGCAGTGAT-3'

mTERT
forward: 5'- GGATTGCCACTGGCTCCG -3'
reverse: 5'- TGCCTGACCTCCTCTTGTGAC -3'

Statistics

Data are expressed as means ± SEM. Significant differences between means were determined using paired t-tests.

Supplemental Figures

Supplemental Figure 1. Cortical loss and hippocampal dysgenesis in p73-/- mice are already present at birth and correlate with prenatal proliferative defects in the SVZ neurogenic zone.

(a, b) By P30, all p73-/- mice (n > 35 mice examined) have various degrees of hydrocephalus, cortical thinning and hippocampal dysgenesis. Cortical thickness is reduced in p73-/- P30 brains (**a**). Five standardized measurements each from 3 brains per genotype were averaged and normalized to WT cortical thickness. **(b)** Hippocampal dysgenesis of p73-/- mice at P30. Note the truncation or absence of the inferior blade of the dentate gyrus (DG). CA1 and CA3 sectors in Ammons horn. Cx, cortex. Hy, hydrocephalus. H&E staining.

(**c**) Defective neurohistologic architecture in p73-/- mice. Tuj1 (β-III tubulin) immunostaining reveals aberrant fiber orientation in the stratum radiatum (SRad) of the CA1-3 layers of the Ammon's horn. While WT CA neurons sent out axons with both coronal and sagittal orientation, all mutant CA axons ran exclusively sagittal and thus appeared cut perpendicularly to coronal sections (left panels). The caudal cortex showed abnormal lamination and mutant axons appeared much shorter than WT axons (right panels). Note, these coronal and sagittal sections of WT and p73-/- brains were taken from the same anatomic level and identical orientation. SPyr, stratum pyramidale.

(**d)** Representative images of E16 WT and p73-/- VZ/SVZ areas stained for Brdu incorporation. Image analysis and quantification of immunohistochemistry was performed with custom-made scripts for 'ImageJ' http://rsbweb.nih.gov/ij/). Data were analyzed using 'R' statistical computing language (http://www.r-project.org).

(**e**) Ki67 immunostaining of the subventricular zone (SVZ) at E18. p73-/- SVZ shows continuous decrease in proliferating precursors. These images are a higher magnification of Figure 1C.

Supplemental Figure 2. p73 is an Essential Regulator of Neural Stem Cell Survival and Self-Renewal

(a) Neurospheres derived from WT brains at E14 and P0 express both TAp73 and ΔNp73 isoforms. While ΔNp73 shows variability, TAp73 is consistently highly expressed. Semiquantitative RT-PCR analysis, GAPDH and Nestin are controls.

(b) Neurospheres derived from WT brains at P0 express higher levels of TAp73 compared to ΔNp73 isoforms at all analyzed passages. GAPDH is shown as control.

Supplemental Figure 3. p73 is an Essential Regulator of Neural Stem Cell Proliferation

(a) Quantification of colonies > 1mm in Neural Colony-Forming Cell (NCFC) Assay in collagen. This assay revealed a decrease in the number of large colonies in E14 NSC cultures already at passage 2.

(b) Size distribution of passage 4 P0 neurospheres derived from SVZ. WT neurospheres tend to accumulate in the upper range, while a substantial number of p73-/- neurospheres accumulate in the lower range. The frequency of their neural stem cells is also markedly reduced compared to WT. A total of > 500 neurospheres were counted per genotype. One WT and two p73-/- mice are shown.

(c) The cell size of dissociated single cells from neurospheres does not differ between WT and p73-/- NSC cultures. FACS analysis.

Supplemental Figure 4. p73-/- Neural Stem Cells Exhibit Impaired S-phase and Increased Senescence, Associated with Deregulation of the Sox and Notch Signaling Pathways of Stem Maintenance

(a) Overlay of Nestin-GFP levels of dissociated neurosphere cells determined by FACS analysis. Of note, at passage 0, WT and p73-/- neurospheres are similarly composed of ~ 65% Nestin-GFP positive cells.

(b) By passage 1, both WT and p73-/- neuropsheres are composed of ~ 80% Nestin-GFP positive cells. No difference in the intensity or % of Nestin-GFP cells was observed between the two genotypes.

(c) Relative mRNA levels Sox2, Sox3, Notch1, Notch3 and Hes5 in *sorted* Nestin-GFP positive (top) and negative (bottom) cells showing dysregulation in these two major pathways of neural stem cell maintenance in passage 1 p73-/- neurospheres derived from P0 brains. Of note, Nestin levels are similar. All values were normalized to GAPDH. All error bars, SEM.

(d) Representative images of Sox2 immunofluorescence analysis of E14 WT and p73-/- NSC.

(e, f) Relative mRNA levels of endogenous Nestin **(e)** and p53 (**f)**. qRT-PCR assays from E14 neurospheres at passage 6. All values were normalized to GAPDH. All error bars, SEM.

(g) Relative mRNA levels of mTERT in sorted P0 Nestin-GFP passage 1 cells. p73-/- neural stem and progenitor cells show a 6-fold decrease in mTERT levels.

Supplemental Figure 5. Impaired Generation of Oligodendrocytes and Neurons from p73-/- Neural Stem Cells

(a) In vitro differentiation assay of dissociated cells from E14 passage 2 neurospheres, shown in Figure 5. At day 7, CNPase-positive cells marking oligodendrocytes were assessed by immunofluorescence for cell number and morphology. Images show the aberrant morphology of many of the generated p73-/- oligodendrocytes. Hoechst counterstain. 40x magnification. **(b)** At day 7, CNPase-positive cells were scored.

(c) While E14-derived NSC at passage 1 still generated equal numbers of Tuj1- positive cells between the two genotypes, E14 p73-/- neurospheres at later passages showed lower numbers of neurons, suggesting an impaired potential to differentiate into neurons.

(d) Abnormal neurons derived from p73-/- P0 neurospheres revealed by Map2a,b, a neuron-specific marker. Note the coiled (arrow) and interrupted (arrow head) processes exhibited by some of the p73-/- neurons. WT is shown for comparison.

Supplemental Figure 6. p73 is also Required in Adult Hippocampal Neurogenesis

(a) Two-weeks neuron birthdating experiment. 6-week old mice were injected 3 times i.p. at 4 hour intervals with BrdU to label neural stem/progenitor cells, located in the subgranular layer (SGZ). Mice were sacrificed two weeks later to determine how many stem/progenitor cells had differentiated into neurons, located in the granule cell layer (GCL) and marked by NeuN positivity (green). Since their BrdU+ label (red) is retained, the newly differentiated neurons appear yellow. Note that p73-/- DG contains far fewer NeuN+ cells (590 per

DG) and BrdU+ cells (321 per DG) compared to WT DG (742 NeuN+ and 522 BrdU+ per DG, respectively) and therefore appears less stained. p73-/- mice show a reduction in the number of double positive cells by 35%. The rare bright yellow cells in the WT image represent multiply labeled cells.

(b,c) No discernable apoptotic activity exists in WT or p73-/- SGZ. Extensive immunostainings for TUNEL **(b)** and cleaved Caspase 3 **(c)** were performed on serially sectioned six week old WT and p73-/- Nestin-GFP brains. (20x) **(b)** Positive control, micrococcal nuclease treated sections from SGZ of WT Nestin-GFP mice stained for TUNEL. Negative control, sections were incubated with Label Solution only (without terminal transferase). (both controls shown as 40x)

(d) To exclude additional neurodegenerative effects that could possibly contribute to the proliferate abnormalities observed in adult hippocampus (see Figure 6), we performed Bielschovsky's silver-staining and phospho-Tau immunostaining to look for plaques and neurofibibrillary tangles. No signs of neurodegeneration could be detected in sections of 6 week-old p73-/- whole brains. Representative sections from silver-stained hippocampus (left) and cortex (right) are shown.

(e) p73-/- mice performed poorly in reflex and neuromuscular function tests (Tail Suspension and Hind Limb Grasping) and sensorimotor and anxiety tests (Open Field and Light/Dark Box) (4), collectively reflecting their severe brain phenotype.

Tail Suspension Test is defined as follows: twisting of the front body toward the hind limbs when suspended by the tail for 2 minutes. Score 2 = all four limbs move symmetrically toward the center of the body and this position is maintained; Score 1 = the mouse moved toward the bat position after several attempts, some uncoordination and slower learning of the position; score 0.5 = attempts to assume the bat position, successful for a very short time; score 0 = the mouse never assumed the bat position.

Hind Limb Grasping Reflex Intensity is defined as follows: The mouse was suspended by its tail and its hind paws were touched with a pen. Strong grip = grasp of foreign object from the first attempt, hold firmly; looser grip = slower reaction, improved in the next attempt; loose grip = slow reaction, improved after the 2-3rd attempt; no grip.

Supplemental References

1. Dimri GP, Campisi J. Molecular and cell biology of replicative senescence. *Cold Spring Harb Symp Quant Biol*. 1994; **59:** 67-73.

2. Dimri GP, Lee X, Basile G, Acosta M, Scott G, Roskelley C *et al.* A biomarker that identifies senescent human cells in culture and in aging skin in vivo. *Proc Natl Acad Sci U S A*. 1995; **92:** 9363-9367.

3. Wolff S, Talos F, Palacios G, Beyer U, Dobbelstein M, Moll UM. The alpha/beta carboxy-terminal domains of p63 are required for skin and limb development. New insights from the Brdm2 mouse which is not a complete p63 knockout but expresses p63 gamma-like proteins. *Cell Death Differ*. 2009; **16:** 1108-1117.

4. Rogers DC, Fisher EM, Brown SD, Peters J, Hunter AJ, Martin JE. Behavioral and functional analysis of mouse phenotype: SHIRPA, a proposed protocol for comprehensive phenotype assessment. *Mamm Genome*. 1997; **8:** 711-713.

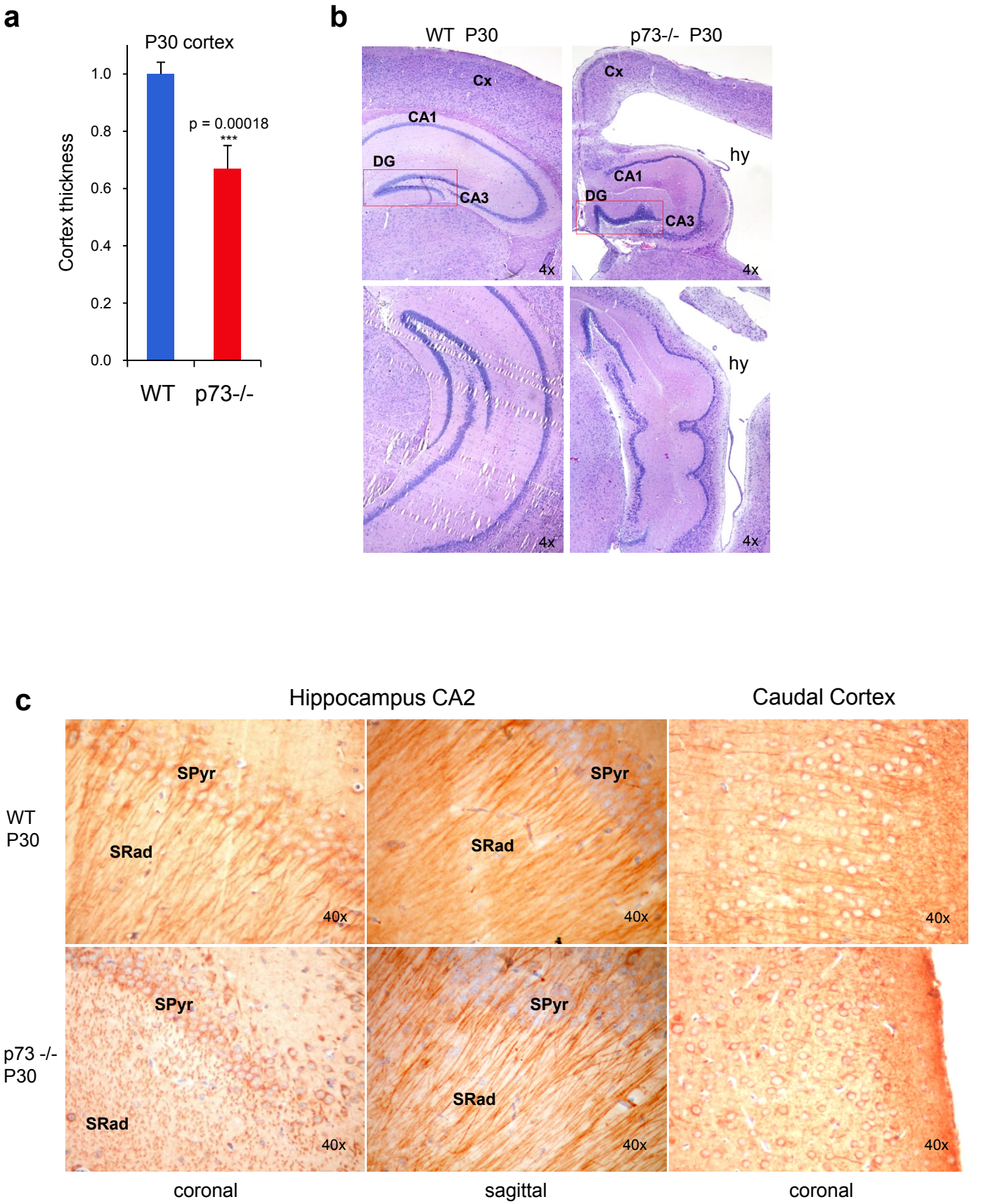

Talos et al., Supplemental Figure 1

d

WT E16

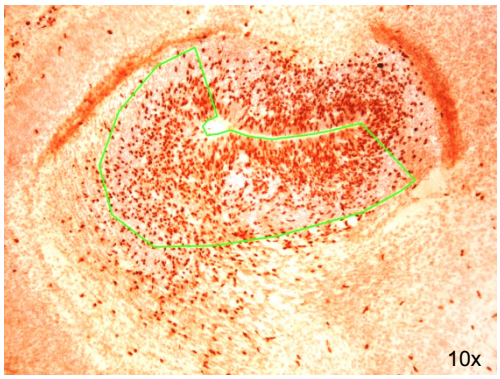

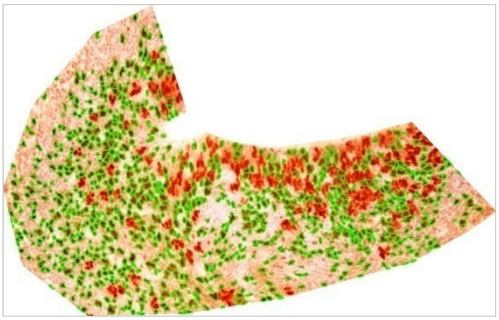

10.3 nuclei/ 10.000 pixels

p73-/- E16

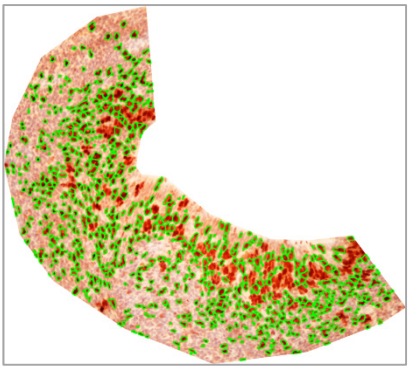

8.8 nuclei/ 10.000 pixels

e

WT E18

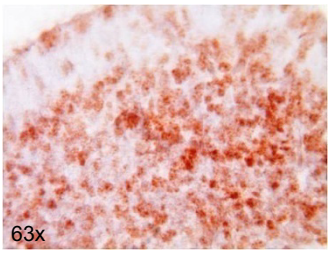

p73-/- E18

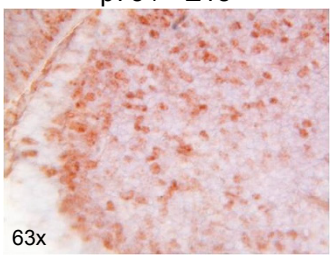

Talos et al., Supplemental Figure 1

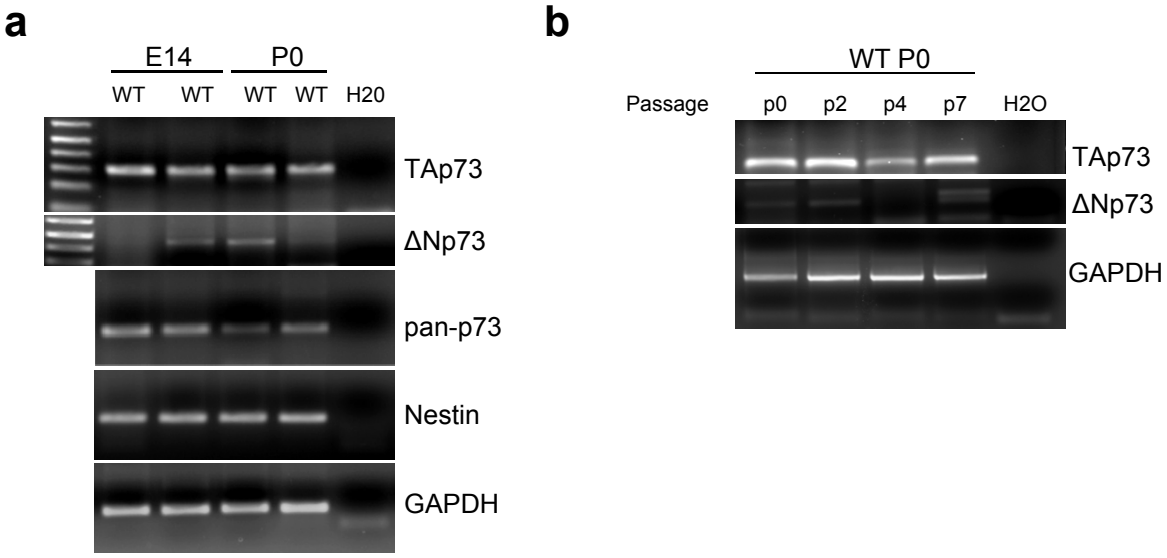

Talos et al., Supplemental Figure 2

a

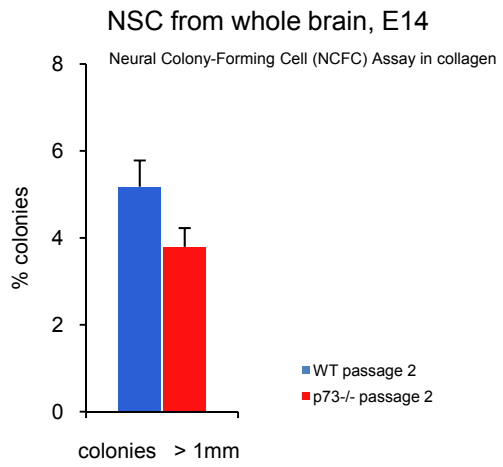

b

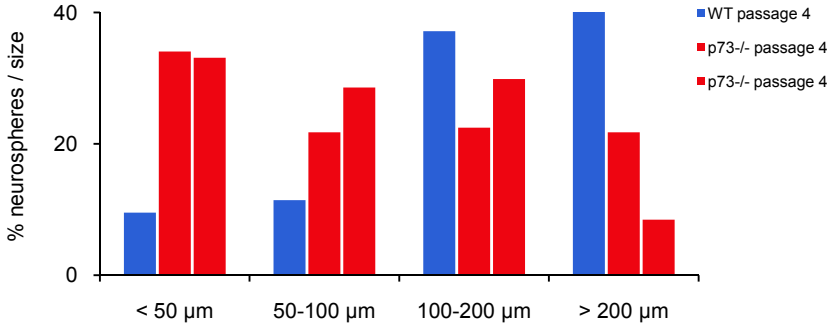

neurospheres	WT	p73-/-	p73-/-
size, µm	171.59 ±7.79	114.09 ±7.06	92.69± 5.31

NSC from SVZ, P0

c

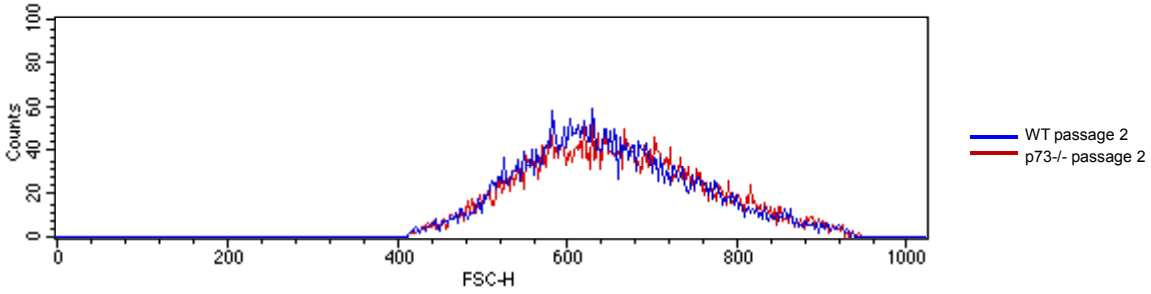

Size of cells from dissociated neurospheres, P0 whole brain

Talos et al., Supplemental Figure 3

a

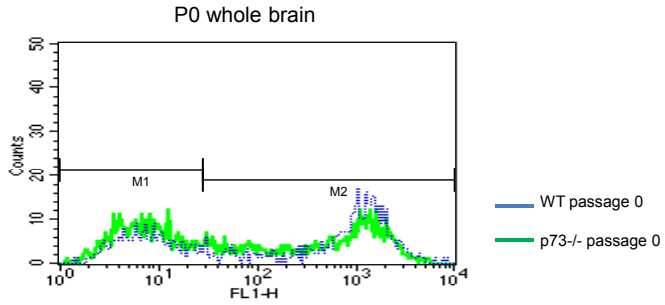

FACS analysis of Nestin-GFP levels

b

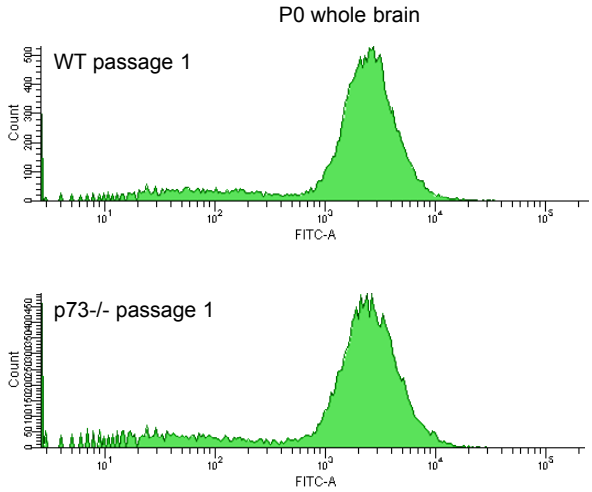

FACS analysis of Nestin-GFP levels

c

Nestin-GFP positive sorted cells

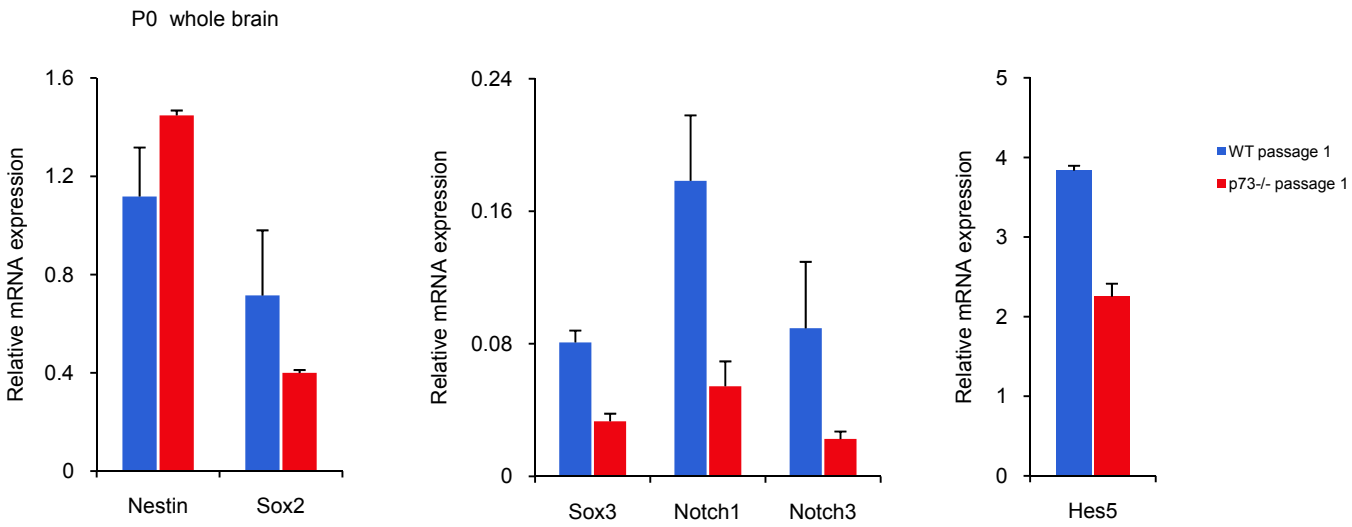

Nestin-GFP negative sorted cells

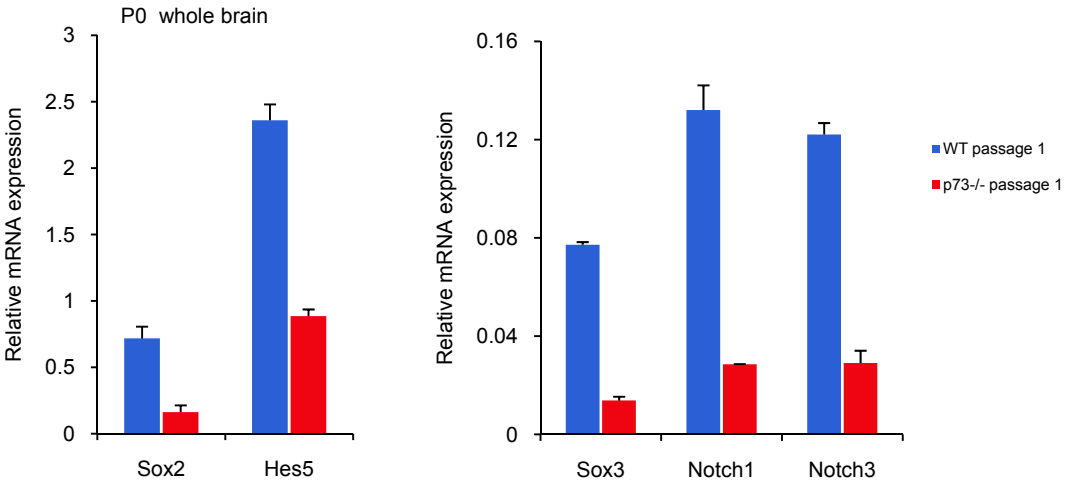

Talos et al., Supplemental Figure 4

d

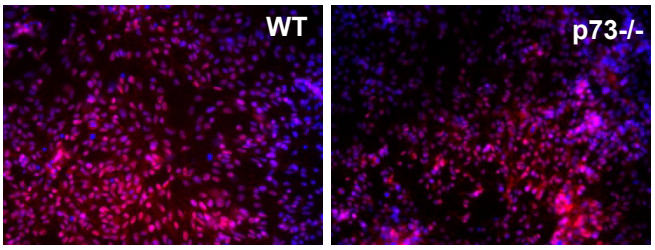

Sox2

e

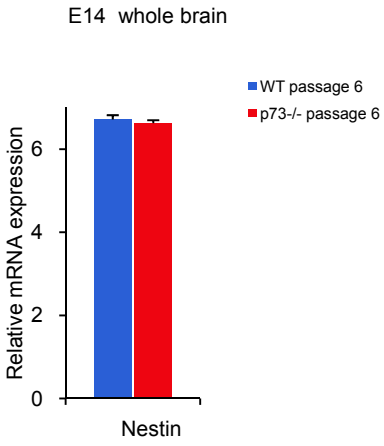

f

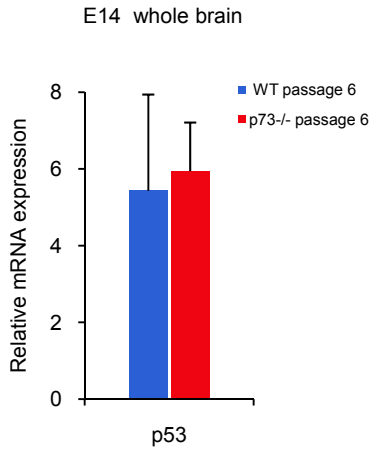

g

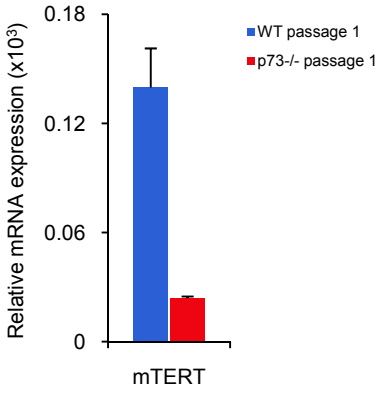

Talos et al., Supplemental Figure 4

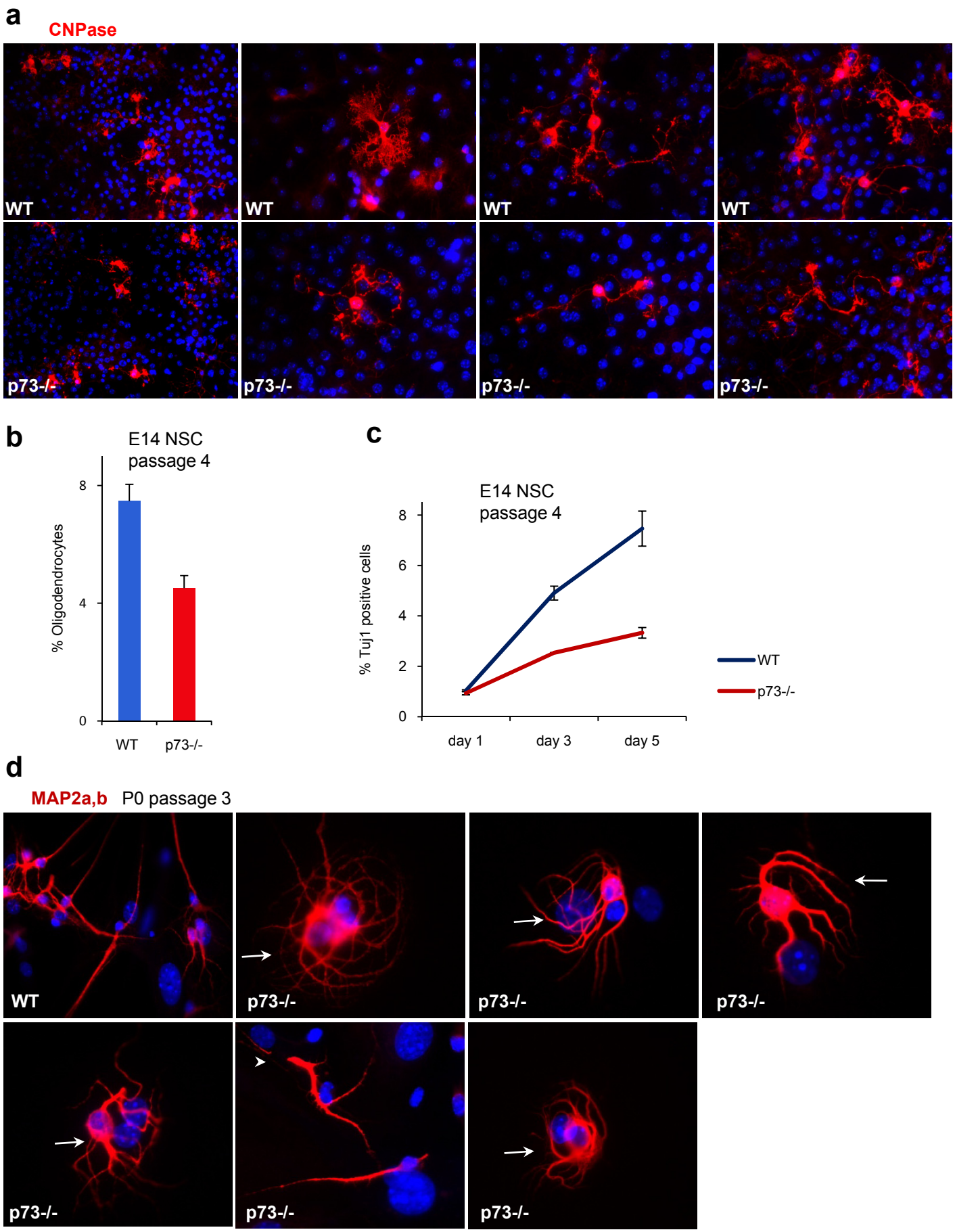

Talos et al., Supplemental Figure 5

a

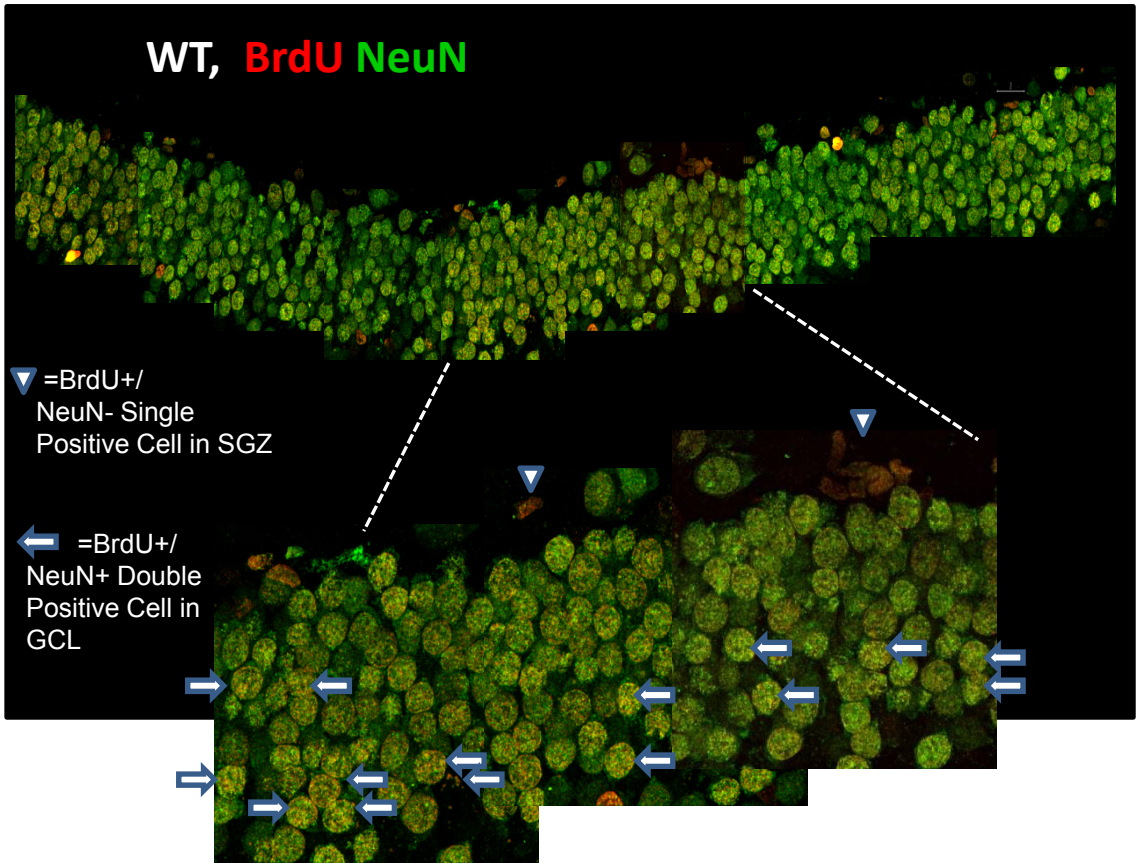

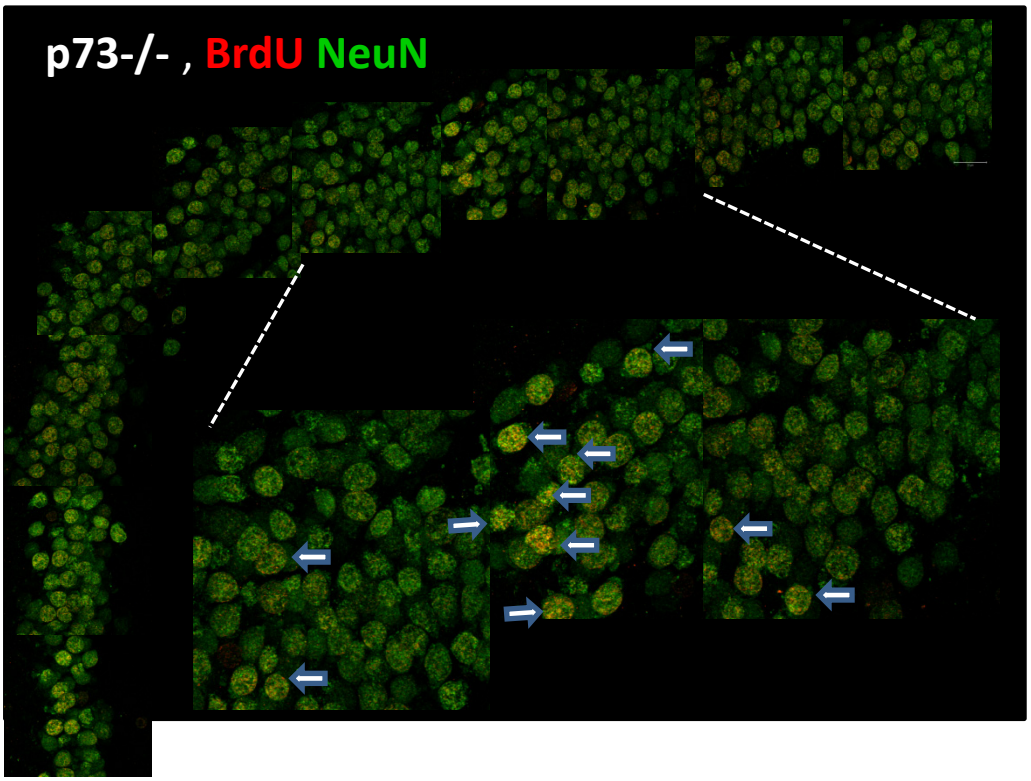

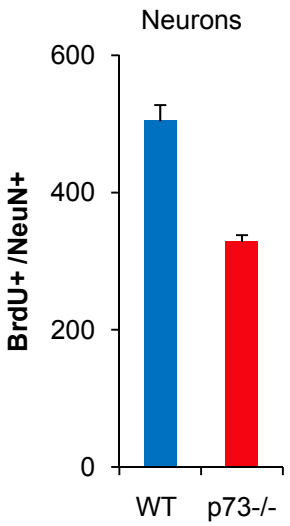

Talos et al., Supplemental Figure 6

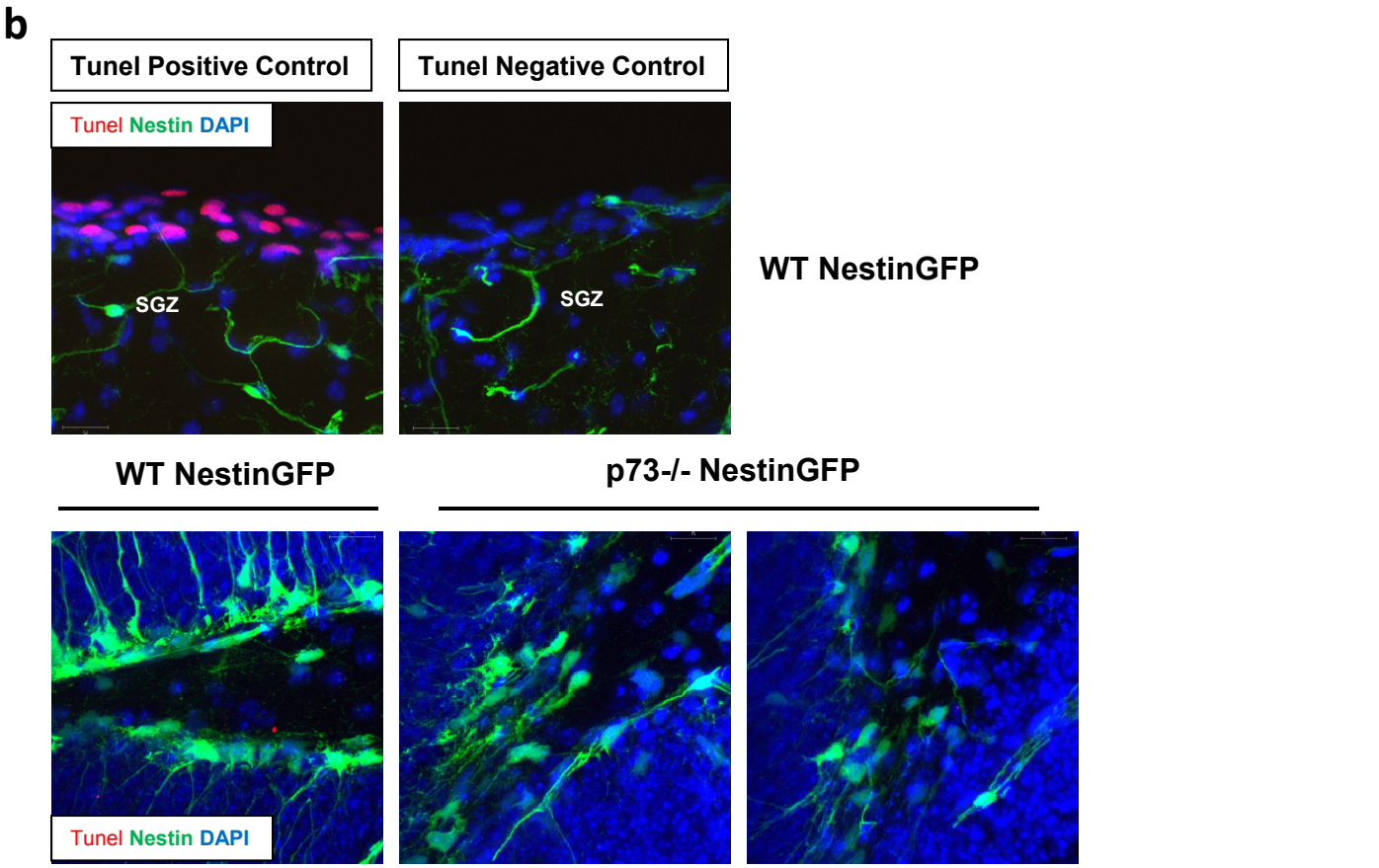

Talos et al., Supplemental Figure 6

d

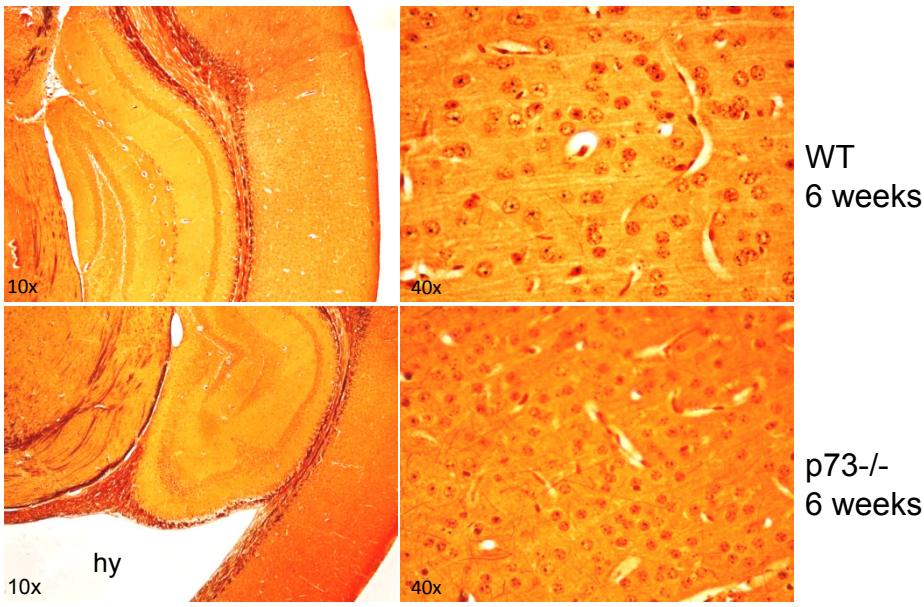

e

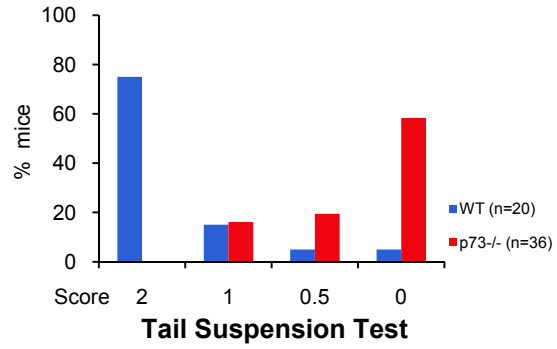

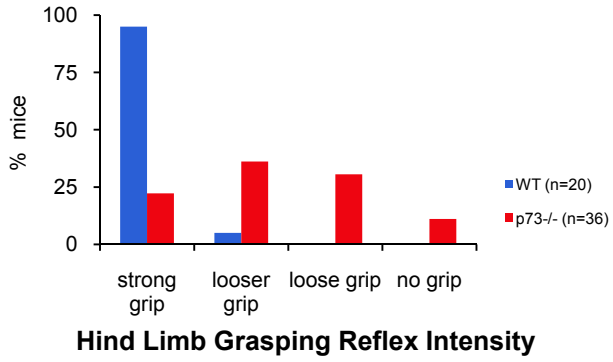

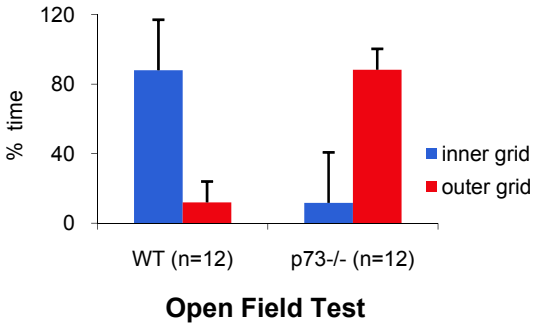

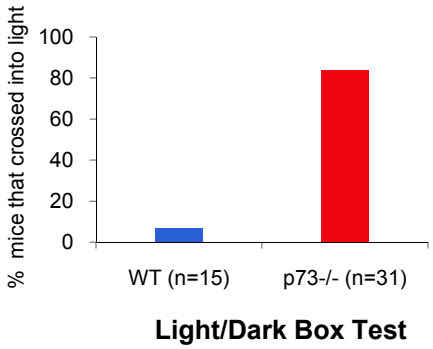

Talos et al., Supplemental Figure 6